23rd ABCM International Congress of Mechanical Engineering
December 6-11, 2015, Rio de Janeiro, RJ, Brazil

DAMAGE MODELS AND CYCLE COUNTING METHODS FOR FATIGUE ASSESSMENT OF POWER PLANT COMPONENTS

Felippe M. S. Costa
PUC-Rio, Rio de Janeiro, Brazil
felippemsc@gmail.com

Jürgen Rudolph
Areva GmbH, Erlangen, Germany
rudolph.juergen@areva.com

José Luiz F. Freire
PUC-Rio, Rio de Janeiro, Brazil
jlfreire@puc-rio.br

José Eduardo Maneschy
JEM Consultoria, Rio de Janeiro, Brazil
emanesc@gmail.com

Abstract. *Structural components of power plants are subjected to thermal transients during their operational life. These thermal transients generate unequal temperature distributions across the wall thickness of the components causing severe thermal stresses. Repetition of transients and consequently repetition of stress and strain variations are responsible for fatigue damage at critical points of the structural components. For these cases, fatigue damage is assessed by calculating the cumulative usage factor CUF. The CUF calculations are based on the stresses and strains histories, on experimental fatigue curves and fatigue damage models, and on algorithms used to determine the number of cycles a given stress or strain range occurs during the life period considered.*

In the present paper, an actual measured load history of pressure and temperature is applied to a thick-walled piping component. This illustrative example is used to present and discuss the fatigue damage model of the ASME code and its association with existing cycle counting models which are applicable to power plant components.

Furthermore, an analytical stress analysis is developed for the previously quoted problem, for that a transient analytical solution proposed earlier by Albrecht was implemented and its results compared with results determined with a commercial finite element software.

Keywords: *Power plant components, design against fatigue, load time histories, cycle counting, non-proportionality.*

1. INTRODUCTION

The methods used to design and to assess considering fatigue as the principal damage mechanism are well treated in references (Sines, Waisman and Dolan, 1959, Bannantine, 1990, Shigley, 2011, Castro and Meggiolaro, 2009) and can be separated into four categories: stress-life methods, strain-life methods, energy-life methods and fracture mechanics methods. The first three methods focus on the study of the initiation of a micro crack, while the last one focuses on the propagation of a macro crack.

Through this paper, some of the aspects of a fatigue analysis using ε−N (strain-life) methods applicable to power plant components submitted to mechanical and thermal loads are developed and discussed.

The first aspect to be studied is the stress analysis of a simple case where a thick walled pipe is submitted to thermal and mechanical loads that are typical for power plant facilities. The principal goal of this study is to develop a procedure that can be implemented in a software in a manner that the time to evaluate the full stress solutions can be optimized, since general finite element procedures implemented so far still show to be too time consuming. This analytical procedure, proposed and applied here in, is not only faster to evaluate but also allows the knowledge of stress distribution across the thickness of the pipes. This distribution is needed to linearize the stresses, so that the ASME and API codes elastic stress fatigue assessment procedures for pressure vessels and for power plant components could be used.

The second aspect is the comparison of two fatigue damage calculation models. Both use the same ASME code elastic model and two cycle counting methods algorithms applicable for load time histories (Simplified Rainflow and Modified Wang Brown). Their characteristics as well as the adaptations necessary to implement calculation procedures are discussed and shown in this paper.

2. STRESS ANALYSIS

The stress analysis is performed for a thick walled pipe submitted to thermal and mechanical loads. This problem is commonly observed in piping and components of thermal power plant facilities. The fluid that flows inside the thick pipe may change its temperature and pressure during operational transients. This creates along each instant of time variation on the mechanical stresses caused by the internal pressure and variation on the thermal stresses caused by the temperature gradient induced in the pipe wall by the change of temperature of the internal fluid.

The resulting mechanical and thermal (elastic) stresses are independent from each other. Because of that, they are calculated separately. The final result is obtained by superposing the results (mechanical plus thermal stresses).

Figure 1 shows the exemplary fluid pressure and temperature time histories that will be used in this paper. These histories start on 15/10/2012 at 15:16 and end on 16/10/2012 at 20:43. They represent the measured history of a generic power plant pipe component that occurred during the plant startup and shut down periods. In the present case, temperature and pressure values were measured and recorded within a 60 second interval.

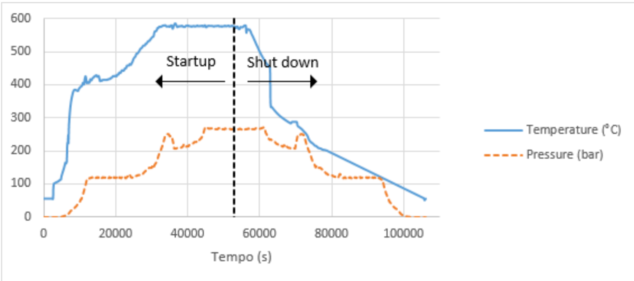

Figure 1. History of temperature and pressure.

The material and geometric properties of the pipe used in this example are: modulus of elasticity (E) = 210 GPa, Poisson's ratio (ν) = 0.3, thermal conductivity (λ) = 33 W/(m·K), coefficient of thermal expansion (α_T) = 12,9·10^{-6} °C^{-1}, specific heat (c) = 622 J/(kg·K), density (ρ) = 7760 kg/m^3, internal radius (r_i) = 100 mm and outer radius (r_o) = 212 mm.

The heat transfer coefficient can be given in terms of a time history. However, in the present paper the coefficient is assumed constant throughout the operation since it did not present a significant variation over the time. The heat transfer coefficient used is equal to 1000 W/m^2·K.

2.1 Mechanical Solution

The mechanical stress solution is given by Lame's equations for thick walled pipes submitted to internal and external pressure:

$$\sigma_r(r) = \frac{p_i r_i^2 - p_o r_0^2}{r_o^2 - r_i^2} - \frac{r_i^2 r_o^2 (p_i - p_o)}{r^2 (r_o^2 - r_i^2)} \tag{1}$$

$$\sigma_\theta(r) = \frac{p_i r_i^2 - p_o r_0^2}{r_o^2 - r_i^2} + \frac{r_i^2 r_o^2 (p_i - p_o)}{r^2 (r_o^2 - r_i^2)} \tag{2}$$

$$\sigma_z = \frac{p_i r_i^2 - p_o r_0^2}{r_o^2 - r_i^2} \tag{3}$$

where r_o and r_i are as defined above, σ_r is the radial stress, σ_θ is the circumferential stress, σ_z is the longitudinal stress, p_o is the external pressure and p_i is the internal pressure (which in the present case is equal to the history of internal pressure shown in Fig. 1).

In Eq. (1) and (2) it is possible to observe that the radial and circumferential stresses are functions of the radial coordinate. Therefore, it is possible to calculate the distribution of the stresses along the thickness of the pipe, which is a prerequisite to perform the stress linearization needed during a fatigue assessment using the ASME code due to the plasticity correction procedure within the simplified elasto-plastic fatigue analysis. Equation (3) is not a function of the radial coordinate because the longitudinal stress is constant along the thickness of the pipe.

Using Lame's equations, the geometric properties of the pipe and the load history presented in Fig. 1, it is possible to calculate the stress components the pipe is submitted to during the startup and shut down periods of the plant. Figure 2 shows the history of the stress components acting on the inner wall of the pipe.

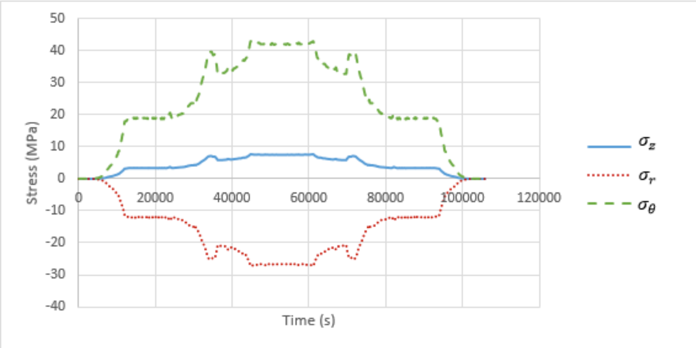

Figure 2. History of mechanical stresses calculated on the inner wall of the pipe.

2.2 Thermal Solution

The thermal solution is not as simple as the mechanical one. Mechanical stresses acting at each time step are a function of the pressure at the respective time step. Thermal stresses acting at each time step are a function of the temperature distribution across the thickness of the pipe at the respective time step. Therefore, it is necessary to calculate the distribution of temperature across the thickness at each time step.

Usually this problem is solved using a finite element analysis. However, the finite element analysis usually consumes a large computational time to evaluate the final result. Because of that, here is proposed an analytical approach developed by Albrecht (Albrecht, 1966). In this paper Albrecht's solution was developed in a manner to end up with a correct and fast evaluation of the thermal stresses involved in this problem.

Since this method is not largely used and its application for the present purpose was not found in the literature, it is necessary to guarantee the validity of the proposed procedure. Thus, the example was solved using a finite element analysis in a manner that the analytical results could be verified by comparison between the two methods.

Albrecht proposed several solutions for this problem (Albrecht, 1966). Only one of those will be used and developed here in. At this solution, before calculating the history of stresses, the distribution of transient temperature along the thickness for each time step is required. This distribution is obtained by the following equation:

$$T(r,t) = T_0 - T_0\pi h \sum_{n=1}^{\infty} \frac{J_0(rk_n)[\lambda k_n Y_1(r_i k_n) + hY_0(r_i k_n)] - Y_0(rk_n)[\lambda k_n J_1(r_i k_n) + hJ_0(r_i k_n)}{(\lambda^2 k_n^2 + h^2) - \dfrac{[\lambda k_n J_1(r_i k_n) + hJ_0(r_i k_n)]^2}{J_1^2(r_0 k_n)}} \cdot e^{-\left(\frac{\lambda}{\rho \cdot c}\right)\cdot k_n^2 \cdot t} \tag{4}$$

where T(r,t) is the temperature as a function of the time (t) in seconds and the radial position (r) in millimeters, T_0 is the initial temperature, and h is the heat transfer coefficient. $J_\alpha(x)$ is the Bessel function of the first kind, $Y_\alpha(x)$ is the Bessel function of the second kind and the n values of k_n are obtained by finding the n (n = 1,2,3,…) roots of the following equation:

$$[\lambda \cdot k_n \cdot J_1(r_i \cdot k_n) + h \cdot J_0(r_i \cdot k_n)] \cdot Y_1(r_o \cdot k_n) - [\lambda \cdot k_n \cdot Y_1(r_i \cdot k_n) + h \cdot Y_0(r_i \cdot k_n)] \cdot J_1(r_o \cdot k_n) \tag{5}$$

With these equations, it is possible to calculate the distribution of temperature along the thickness of a thick walled pipe. A numerical solution algorithm was implemented to calculate the distribution. The flowchart of this numerical solution can be seen in the Annex.

After calculating the temperature distribution along the thickness, the stresses are calculated using equations (6), (7) and (8):

$$\sigma_r(r,t) = \frac{\alpha_T E}{1-\nu}\left[\frac{r^2 - r_i^2}{r^2(r_o^2 - r_i^2)}\int_{r_i}^{r_o} T(r,t)\cdot r \cdot dr - \frac{1}{r^2}\int_{r_i}^{r} T(r,t)\cdot r \cdot dr\right] \tag{6}$$

$$\sigma_\theta(r,t) = \frac{\alpha_T E}{1-\nu}\left[\frac{1}{r^2}\int_{r_i}^{r} T(r,t)\cdot r \cdot dr + \frac{r^2 + r_i^2}{r^2(r_o^2 - r_i^2)}\int_{r_i}^{r_o} T(r,t)\cdot r \cdot dr - T(r,t)\right] \tag{7}$$

$$\sigma_z(r,t) = \frac{\alpha_T E}{1-\nu}\left[\frac{2}{r_o^2 - r_i^2}\int_{r_i}^{r_o} T(r,t)\cdot r\cdot dr - T(r,t)\right] \tag{8}$$

Since the values of the temperature along the thickness are obtained discretely, the integrations are solved using the trapezoidal rule. With the explained procedure and knowing the geometric and material properties and the given history of temperature, the circumferential stress history was calculated for the startup period and the results were compared with the results obtained using a finite element model (Figure 3).

Figure 3. History of the circumferential stress during the start up period.

Analytical and finite element results were similar. The largest difference between the solutions can be observed at the circle marked in Fig. 3. At this instant time, the stress values are the highest, and it is possible to notice that the analytical solution gives results slightly more conservative than the FE solution.

Based on the facts that the analytical solution allows stress linearization and that is faster to obtain the final results (consumed 1/3 of the time when compared with the FE solution), it is concluded that the proposed analytical solution can be advantageously used in the component fatigue assessment as long as the thick walled pipe geometry idealization holds true.

3. DAMAGE MODELS

Fatigue damage models relate strain or stress ranges or energy variables to the number of cycles they actuate until a crack is initiated. The damage model used herein is the one present in the ASME code that performs a fatigue assessment using an elastic stress analysis.

3.1 Fatigue Design Curves

A fatigue analysis made using the ASME Boiler and Pressure Vessel Code (ASME, 2010a, ASME, 2010b) has to use the fatigue curves presented in the code. The fatigue curves of the ASME code are derived from results of experimental tests. Unnotched and polished standard specimens without welds are submitted to fully reversed (R=-1.0) strain controlled tests at room temperature. The results alternated stress (S_a) x number of cycles to failure (N) are plotted in a log-log scale chart, where the alternating stress is the value of half the strain range ($\Delta\varepsilon/2$) multiplied by Young's modulus of the steel.

The failure of those specimens is defined at the time that the alternate tensile load drops 25% of its test steady value (Rettenmeier, Herter, Schuler and Fesich, 2014). The number of cycles to failure is the number of cycles necessary to present this stress drop. The specimens used are usually cylindrical and have between 9 and 12 mm of diameter, so this stress drop represents a crack of approximately 3 mm of depth (Rettenmeier, Herter, Schuler and Fesich, 2014).

The fatigue curves in the ASME code result from the best-fit curves obtained from the experimental results (O'Donnell, 2009). The design fatigue curves presented in the code originally considered margins of 2 on the stress and 20 on the cycles(Cooper, 1992) . These margin factors are introduced in order to take into consideration effects that change the fatigue strength of components such as "scatter of data (minimum to mean) and material variability", "size effects", "surface finish and environment" (Cooper, 1992) where "environment" designated the laboratory environmental conditions. Mean stress effects are considered by a modified Goodman correction procedure. In (Chopra, 2007) the factor on strain respectively stress amplitude is (conservatively) estimated to S = 2.0 and additionally a mean stress correction is applied: The best-fit curves are first corrected for mean stress effects by using the modified Goodman relationship, and the mean-stress adjusted curve is reduced by a factor of 2 on stress or 12 on cycles, whichever is more conservative. The new design curve for austenitic stainless steels in the ASME-Code, App I (ed. 2010 and following) is based on (Chopra, 2007). Other international design codes follow up these developments, e.g. the German Nuclear Safety Standard KTA (Schuler, 2013).

3.2 Fatigue Assessment Using Elastic Stress Analysis (Simplified elasto-plastic fatigue analysis)

This method requires the calculation of two types of stresses: S_n, which is a result of the stress linearization procedure (explained below) and S_p, which is the total stresses. The method is applied to each range of stress. The stress ranges are calculated using the stresses that occur at the beginning and at the end of each stress cycle. For each stress cycle the ASME code[1] gives two load points in the time history: ${}^{m}t$ and ${}^{n}t$. Using these points it is possible to calculate the stress ranges ΔS_p for the time-cycle being considered:

$$\Delta S_p = \frac{1}{\sqrt{2}}\left[\left(\Delta\sigma_{xx} - \Delta\sigma_{yy}\right)^2 + \left(\Delta\sigma_{xx} - \Delta\sigma_{zz}\right)^2 + \left(\Delta\sigma_{yy} - \Delta\sigma_{zz}\right)^2 + 6\left(\Delta\tau_{xy}{}^2 + \Delta\tau_{xz}{}^2 + \Delta\tau_{yz}{}^2\right)\right]^{0.5} \quad (9)$$

where:

$$\Delta\sigma_{ij} = \left|{}^{m}\sigma_{ij} - {}^{n}\sigma_{ij}\right| \quad (10)$$

The alternating stress is then defined as:

$$S_a = \frac{K_f K_e \Delta S_p}{2} \quad (11)$$

where K_f is the fatigue strength reduction factor and K_e is the fatigue penalty factor. The value of the fatigue strength reduction factor is one if the stresses calculated already had taken in consideration the effects of a local notch or weld. If this is not the case, the value of K_f must be calculated.

The value of K_e depends on the S_n stress range. The range of the S_n stress, is calculated similarly to the range of the S_p stress- using Eq. (9). The difference is that the stress range S_n considers only the linearized summation of the stresses. The value of K_e is then obtained by using the following equation:

$$\begin{cases} K_e = 1 & for \quad \Delta S_n \le S_{PS} \\ K_e = 1 + \dfrac{(1-n)}{n\cdot(m-1)}\cdot\left(\dfrac{\Delta S_n}{S_{PS}} - 1\right) & for \quad S_{PS} < \Delta S_n < m\cdot S_{PS} \\ K_e = \dfrac{1}{n} & for \quad \Delta S_n \ge m\cdot S_{PS} \end{cases} \quad (12)^2$$

where the values of m and n are material properties and the value of S_{PS} is the maximum value between three times the average value of the allowable stress at the highest and lowest temperature occurring in the cycle, and two times the average value of the yield stress on the highest and lowest temperature occurring in the cycle as given by the equations described in Fig. 5. The values of m and n are given in ASME code for different materials and their values vary from 1.7 to 3 for m and from 0.2 to 0.3 for n.

The advantage of this method is that, with the inclusion of the fatigue penalty factor, it is possible to perform a fatigue evaluation of a component under cyclic plasticity employing elastic stress analysis. It is possible to notice in

[1] This definition is given in the ASME code. In Section III, S_n and S_p are determined using the Tresca criterion. On the other hand, in Section VIII these quantities are obtained by the von Mises criterion.

[2] This equation is defined in the ASME code Section VIII. In Section III, the S_{PS} is replaced by S_m, which is also a material property .

equation (12) that the value of K_e varies between 1.0 and 3.3 or 5.0 (depending on the value of n). This constitutes the simplified elasto-plastic fatigue analysis.

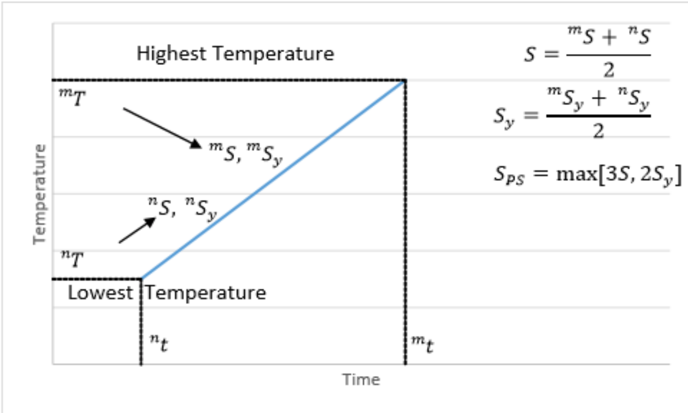

Figure 5. Exemplification of the calculation of S_{PS}.

3.3 Stress Linearization

The stress linearization method is used here to obtain the S_n and S_p stresses. The application of a stress linearization process through the thickness of a specific section of the component enables the determination of the linearized membrane and bending as well as peak stress components, the S_n stress resulting from the summation of membrane and bending components and S_p resulting from the summation of membrane, bending and peak stresses. The linearized stress components can be calculated using the following equations:

$$\sigma_{ij,m} = \frac{1}{tk}\int_0^{tk} \sigma_{ij} dx \tag{13}$$

$$\sigma_{ij,b} = \frac{6}{tk^2}\int_0^{tk} \sigma_{ij}\left(\frac{tk}{2} - x\right) dx \tag{14}$$

$$\sigma_{ij,P}(x)\,|_{x=0} = \sigma_{ij}(x)\,|_{x=0} - (\sigma_{ij,m} + \sigma_{ij,b}) \tag{15}$$

$$\sigma_{ij,P}(x)\,|_{x=tk} = \sigma_{ij}(x)\,|_{x=tk} - (\sigma_{ij,m} - \sigma_{ij,b}) \tag{16}$$

where t_k is the thickness of the selected cross section. Equation (13) calculates the membrane stress ($\sigma_{ij,m}$) along the ij direction, Eq. (14) calculates the bending stress ($\sigma_{ij,b}$) along the ij direction and Eqs. (15) and (16) calculate the peak stress ($\sigma_{ij,P}$) along the ij direction at the inner and outer wall locations respectively.

Since the analytical solutions proposed in the stress analysis are functions of the radial position, the trapezoidal rule is used to solve the integrations in Eqs. (13) and (14) applied to the most critical point which is found to be located in the pipe inner wall. Results are presented in Fig. 6.

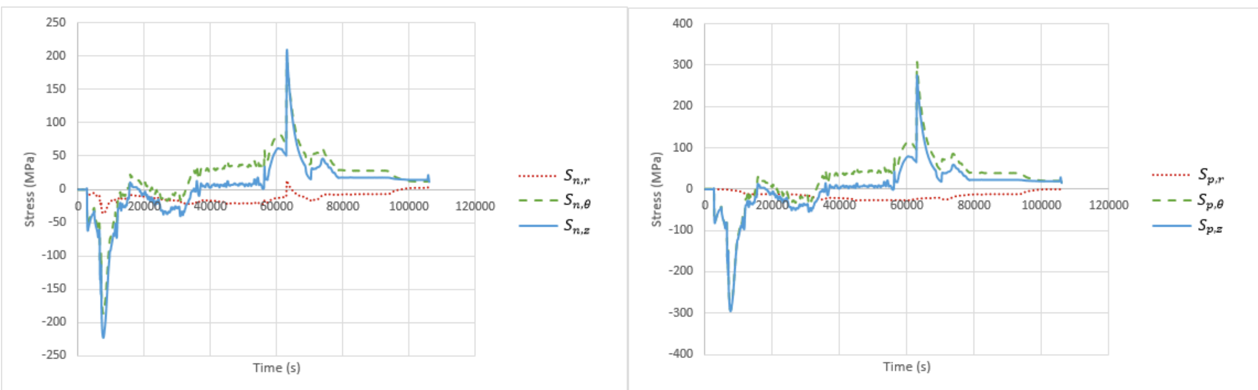

Figure 6. History of the S_n and S_p stresses caused by thermal plus mechanical loads.

4. CYCLE COUNTING METHODS

There are several cycle counting methods available in the current literature in order to identify damage relevant cycles. The present paper focuses two methods: the Simplified Rainflow and the Modified Wang Browm (MWB) methods. It is important to highlight that the ASME code allows the use of the Simplified Rainflow only in cases where the loading is proportional (the direction of the principal stresses does not change with time). When loads are non-proportional, the code recommends to use the Extreme Value Method (or Max-Min).

A known phenomenon that occurs when the linearized stresses are used in a fatigue analysis is that sometimes the peak (or valley) of the stress components of the tensors S_p and S_n do not take place at the same time step. In the ASME code the alternating stress S_a (the parameter to enter in the fatigue curve) is a function of the values of K_e and of the range of S_p (determined by using one cycle counting method) - equation (15). K_e is a function of the range of S_n and of the material properties as it is shown in equation (16).

To form the stress ranges the cycle counting is carried out using the S_p stresses. The ranges of S_n are calculated using the same time steps that generated the S_p ranges. In that way, if a cycle counting routine returns the range of S_p using the time steps ${}^{m}t$ and ${}^{n}t$, the range of S_n is calculated using the time steps ${}^{m}t$ and ${}^{n}t$.

However, this leads to a problem: in some cases, performing the cycle counting using the history of S_p stresses may result in a non-conservative fatigue analysis. The cycle counting will return the time steps that creates the biggest ranges for the S_p stresses, which is not necessarily the time steps that create de biggest values of S_a. In order to avoid these non-conservative results, the highest value of the alternating stress has to be found on the cycle counting method. The developed methods to avoid this problem are better clarified along with the explanation of each cycle counting method.

4.1 Simplified Rainflow

The Simplified Rainflow is the Rainflow Method presented in the ASME Code Section VIII, Division 2, Annex 5.B. It modifies the regular Rainflow by previously re-ordering the load history so that it begins and ends with either the highest peak or the lowest valley. This re-ordering eliminates the necessity of counting half cycles, and only full cycles are counted automatically. Its use for non-proportional loadings can be done by making two modifications.

In the first modification the cycle counting is applied to each stress component. Peaks and valleys belonging to the selected cycle counting stress direction determine the time steps where stress values are to be taken from the other stress components in order to calculate the equivalent stress compatible with the original counting. Therefore, there will be as many counts as stress components. The counting that gives the maximum fatigue damage is selected to represent the final damage.

In the second modification the stress range is no longer calculated as the modulus of the difference between values occurring at the start and final points of each cycle counted. The range is calculated using all stress components for each cycle counted. The ranges are calculated using the von Mises equivalent or Tresca criteria. Equation (9) is an example of equivalent ranges to be calculated using the von Mises criterion.

To be sure that the highest value of alternating stress is found a simple method is proposed here. The method consists in, after the cycle counting is performed, a search for the combinations of time steps - close to the time steps counted – that will generate the largest alternating stress is performed. Since the cycle counting procedure is implemented using a software, the number of time steps in the search to be considered before and after the time step counted along the routine application (the so-called rubber band) is one of the input parameters that needs to be given by the user. A similar rubber band methodology is proposed in the EPRI document (EPRI, 2011).

For example, if the Simplified Rainflow routine returns the time steps ${}^{m}t$ and ${}^{n}t$ and the calculation enclosure is composed by three loads steps before and four loads steps after, the time step counted. The search for the biggest alternated stress is made by calculating all the possible alternating stress values obtained with the combinations of the time steps between ${}^{m-3}t$ and ${}^{m+4}t$, with the time steps between ${}^{n-3}t$ and ${}^{n+4}t$. The combination that returns the largest value of the alternating stress is the final result for the considered time step. As a consequence, the number of time steps defined by the user has an important influence on the result.

This number cannot be too low, because in that way the maximum alternating stress will not be found. It cannot be too high, because not only the time to run the evaluation procedure will increase drastically, but also because it is possible to reach another peak or another valley which will produce an erroneous cycle counting result.

4.2 Modified Wang Brown (MWB)

Even with these modifications, the Simplified Rainflow is not seen in the literature as the best cycle counting method to deal with non-proportional loading. Some other methods are more recommended in such cases. For example, as it was already mentioned, the ASME code recommends to use the Extreme Value Method. However, this method can generate non-conservative results (Socie and Marquis, 1999). Consequently, in the present paper the modified MWB method, as proposed by Meggiolaro and Castro (2012b), is the subject of a more detailed consideration.

The first step of this method consists of a conversion of the entire history of stresses to a five dimensional Euclidian space: ($P_i = (S_1, S_2, S_3, S_4, S_5)$). The dimensional reduction is accomplished by the following equations:

$$S_1 \equiv \sigma_{xx} - \frac{\sigma_{yy}}{2} - \frac{\sigma_{zz}}{2},\ S_2 \equiv \frac{\sigma_y - \sigma_z}{2}\sqrt{3},\ S_3 \equiv \tau_{xy}\sqrt{3},\ S_4 \equiv \tau_{xz}\sqrt{3},\ S_5 \equiv \tau_{yz}\sqrt{3} \tag{17}$$

The second step consists of finding in the history the pair of points that are farthest away from each other. Having determined these points, the one with that has the greatest distance to the origin is chosen. This is the point where the cycle counting starts. The third step considers the point under consideration as the initial point of the cycle counting (P_i). Then, the final point (P_f) is found when a point with the biggest distance in relation with P_i is found, or when a segment from a previous count is found. After that a half cycle is counted from P_f to P_i, and the routine goes to the next point and returns to the third step until every point is already counted.

After the cycles are counted, the authors (Meggiolaro and Castro, 2012b) recommended using an enclosing surface solution fitting the full and half cycles in order to calculate the parameters needed to obtain the fatigue damage associated with each cycle. After that, in order to evaluate the total damage, a damage accumulation rule (Miner's rule for example) is adopted.

Since the damage model used herein is the one cited previously, the enclosing surface solution must give an equivalent range of ΔS_p and ΔS_n. The enclosing surface solution chosen is the minimum ball, and its use can be observed in Fig. 7.

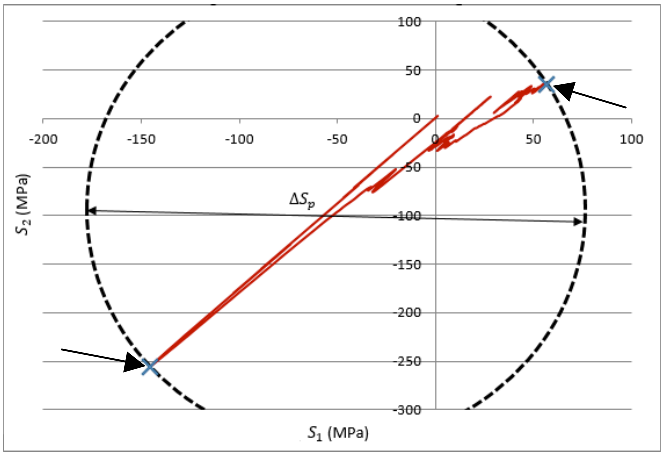

Figure 7. Example on the calculation of the S_p range using the minimum ball method.

To obtain this figure, the history of S_p stresses shown in Fig. 6 was reduced to a five dimensional Euclidian space using Eq. 17. After that the cycle counting returns the path between the points marked with an arrow. The minimum ball solution is then used to calculate the range of ΔS_p, where this range is the diameter of the minimum ball that circumscribes the entire path between the points marked with an arrow. To find the range of ΔS_n, the procedure is analogous. Since the cycle counting routine returns the time steps of the history based on the history of the S_p stresses, it is possible to access the value of the S_n stresses at each one of these time steps and reproduce Fig. 7 for the S_n stresses.

To be sure that the highest value of the alternating stress is found, a similar method is proposed for this cycle counting method. The time steps relative to the points that are touching the minimum ball (for example, in Fig. 7 the points marked with an arrow) are obtained, then the same procedure is followed. A combination of all the time steps inside of the calculation enclosure is made to search for the pair of time steps that will return the biggest value of the alternated stress.

5. APPLICATION EXAMPLE

The thermal-pressure loading history considered previously in Fig. 1 and applied to the structural pipe using the Albrecht-Lamé stress solutions resulted in the history of stresses given in Fig. 6. A stainless steel was adopted as model material. The fatigue curve is given in the ASME code (see section 3.1of this paper). Fatigue damage was determined using both cycle counting methods explained above. The results of the cycle counting routines (Simplified Rainflow and MWB) returned that only one cycle was counted as significant, since it was the only one that gave a CUF value above zero. In other words, the other cycles counted resulted in insignificant or null CUF values. Consequently, the outputs generated using both cycle counting methods were identical: ΔS_p was equal to 607.53 MPa, ΔS_n was equal to

362.09 MPa, K_e was equal to 1.26, and consequently the alternating stress (S_a) was equal to 433.82 MPa, resulting in a CUF value equal to 0.000176.

The fact that the loading history used in this example has characteristics of maintaining principal directions constant and low non-proportionality among the stress components also influences similar results for both methods. Nevertheless it has to be observed that load histories that are multiaxial and highly non-proportional may result in non-conservative results if the Simplified Rainflow method is used (Costa, 2015).

Therefore, as the Simplified Rainflow and the Extreme Value Method (Socie and Marquis, 1999) may result in non-conservative results depending on the characteristics of the load history and as it seems that the simplified elasto-plastic fatigue analysis based on elastic stress analysis and plasticity correction will remain the mostly applied method on an engineering calculation level, the advantages of more complex cycle counting methods should be pointed out and the applicability of the Modified Wang-Brown solution as a standard fatigue post processing method should be better comprehended and implemented.

6. CONCLUSIONS

This paper calls attention to and put together three actions to enhance the calculation of fatigue damage of thick walled pipe components that are submitted to complex load histories of thermal transients combined with constant or varying internal pressure. It firstly showed that an analytical solution may be used to determine stress component profiles along the thickness of pipes under thermal transients. Secondly, it showed that the elastic solution enables the determination of linearized stresses that are requested by the elastic fatigue damage solution used by the ASME Code, sections III and VIII, to be applied in cases where elastic-plastic stresses are present. Thirdly, it presented procedures to use two cycle counting methods to be coupled to the code fatigue damage model for cases where non-proportional loading is present.

In future work, realistic complex temperature transients are to be examined with regard of the degree of non-proportionality of the resulting stress-time histories. These studies can advantageously be based on the analytical transient temperature and stress solution presented in this paper.

7. REFERENCES

Albrecht, W. (1966). Instationäre Wärmespannungen in Hohlzylindern. *Konstruktion*, *18*(6), 224-231.

ASME (The American Society of Mechanical Engineers), (2010a), ASME Boiler and Pressure Vessel Code, Section III, Edition 2010.

ASME (The American Society of Mechanical Engineers), (2010b), ASME Boiler and Pressure Vessel Code, Section VIII, Edition 2010.

Bannantine, J. (1990). Fundamentals of metal fatigue analysis. *Prentice Hall, 1990,*, 273.

Castro, J. T. P. D., & Meggiolaro, M. A. (2009). Fadiga: técnicas e práticas de dimensionamento estrutural sob cargas reais de serviço. Volume I-Propagação de Trincas, Efeitos Térmicos e Estocásticos".

Chopra, O., Shack, W.J. (2007). Effect of LWR Coolant Environments on the Fatigue Life of Reactor Materials. NUREG/CR-6909, ANL-06/08, February 2007.

Cooper, W.E. (1992). The initial scope and intent of the section III fatigue design procedures. WRCB, Technical Information from Workshop on Cyclic Life and Environmental Effects in Nuclear Applications, Clearwater, Florida, 1992.

Costa, F. M. S. (2015). Cycle counting methods for load-time-histories typical for power plant applications. Masters Dissertation, PUC-Rio, 2015

EPRI corporate document: *Stress-Based Fatigue Monitoring: Methodology for the Fatigue Monitoring of Class 1 Nuclear Components in a Reactor Water Environment.* EPRI, Palo Alto, CA: 2011. 1022876.

Meggiolaro, M. A., & de Castro, J. T. P. (2012a). An improved multiaxial rainflow algorithm for non-proportional stress or strain histories–Part I: Enclosing surface methods. International Journal of Fatigue, 42, 217-226.

Meggiolaro, M. A., & de Castro, J. T. P. (2012b). An improved multiaxial rainflow algorithm for non-proportional stress or strain histories–Part II: The Modified Wang–Brown method. *International Journal of Fatigue*, *42*, 194-206.

O'Donnell, W. J. (2009). Code Design and Evaluation for Cyclic Loading—Sections III and VIII. *Companion Guide to the ASME Boiler and Pressure Vessel Code*, *2*.

Rettenmeier, P., Herter, K. H., Schuler, X., & Fesich, T. M. (2014). Application of Advanced Fatigue Damage Parameters in Comparison With Fatigue Analysis Included in Codes and Standards. In *ASME 2014 Pressure Vessels and Piping Conference* (pp. V003T03A058-V003T03A058). American Society of Mechanical Engineers.

Rudolph, J., Maneschy, J. E., Cisternas, M., Freire, J. L. F., Costa, F. M., & Silva, B. (2014). Fatigue Assessment of NPP Piping and Components Using Realistic Thermal-Mechanical Load Histories. In *ASME 2014 Pressure Vessels and Piping Conference* (pp. V001T01A039-V001T01A039). American Society of Mechanical Engineers.

Schuler, X., Herter, K.-H., Rudolph, J. (2013): Derivation of design fatigue curves for austenitic stainless steel grades

1.4541 and 1.4550 within the German Nuclear Safety Standard KTA 3201.2. *Proceedings of PVP2013. Paper No. PVP2013-97138. 2013 ASME Pressure Vessels & Piping Division Conference. July 14-18, 2013, Paris, France.*
Budynas R. D. & Nisbeett, J. K. (2011). *Shigley's mechanical engineering design*. McGraw-Hill Education.
Sines, G., Waisman, J. L., & Dolan, T. J. (Eds.). (1959). *Metal fatigue*. McGraw-Hill.
Socie, D., & Marquis, G. (1999). Multiaxial fatigue. *Warrendale, PA: Society of Automotive Engineers, 1999. 502*.

8. RESPONSIBILITY NOTICE

The authors are the only responsible for the printed material included in this paper.

9. ANNEX

Flowchart of the algorithm that solves the Albrecht's analytical solution.